Received 28 June 2018; accepted 18 July 2018. Date of publication 11 April 2018; date of current version 31 August 2018.
The review of this paper was arranged by Editor N. Collaert.

*Digital Object Identifier 10.1109/JEDS.2018.2861622*

# Ultrahigh-Sensitive CMOS pH Sensor Developed in the BEOL of Standard 28 nm UTBB FDSOI

**GETENET TESEGA AYELE [1,2,3,4], STEPHANE MONFRAY [1], SERGE ECOFFEY [3,4], FRÉDÉRIC BOEUF [1], JEAN-PIERRE CLOAREC [2], DOMINIQUE DROUIN [3,4] (Member, IEEE), AND ABDELKADER SOUIFI [2]**

1 Advanced Devices, STMicroelectronics, 38920 Crolles, France
2 Electronic Devices, INL, 69100 Villeurbanne, France
3 Institut interdisciplinaire d'innovation technologique, Université de Sherbrooke, Sherbrooke, QC J1K 2R1, Canada
4 Laboratoire Nanotechnologies Nanosystèmes CNRS UMI-3463, Université de Sherbrooke, Sherbrooke, QC J1K 2R1, Canada

CORRESPONDING AUTHOR: G. T. AYELE (e-mail: getenet-tesega.ayele@insa-lyon.fr)

**ABSTRACT** This paper reports ultrahigh-sensitive and ultralow-power CMOS compatible pH sensors that are developed in the back-end-of-line (BEOL) of industrial 28-nm ultrathin body and buried oxide (UTBB) fully depleted silicon-on-insulator (FDSOI) transistors. Fabricating the sensing gate and the control gate of the sensors in a capacitive divider circuit, CMOS compatible pH sensors are demonstrated where the front gate bias is applied through a control gate rather than a bulky reference electrode. On the other hand, the strong electrostatic coupling between the front gate and the back gate of FDSOI devices provide an intrinsic signal amplification feature for sensing applications. Utilizing an atomic layer deposited aluminum oxide ($Al_2O_3$) as a pH sensing film, pH sensors having a sensitivity of 475 mV/pH and 730 mV/pH in the extended gate and BEOL configuration, respectively, are reported. Sensitivities of both configurations are superior to state-of-the-art low power ion-sensitive field-effect transistors. The small sensing area and the FDSOI-based low power technology of the device make the sensors ideal for the IoT market. The proposed approach has been validated by TCAD simulation, and demonstrated through experimental measurements on proof-of-concept extended gate pH sensors and on sensors that are developed in the BEOL of industrial UTBB FDSOI devices.

**INDEX TERMS** Aluminum oxide, back-end-of-line (BEOL), capacitive coupling, extended gate, fully-depleted silicon-on-insulator (FDSOI), ion-sensitive field-effect transistor (ISFET), pH sensor.

## I. INTRODUCTION

The development of an ion-sensitive solid state device, commonly called as ISFET (ion-sensitive field-effect transistor), that combines the principles of an MOS transistor and a glass electrode was introduced by P. Bergveld in 1970 [1]. The concept was based on the principle that ionic species incorporated in the device during fabrication of metal-oxide-semiconductor field-effect transistor (MOSFET) introduce variations in the threshold voltage ($V_{th}$) [2]. ISFETs employ this effect in a reproducible and reversible form to measure the activity of an ionic species in an aqueous solution to which the gate insulator is exposed [2]. The structure of these sensors is similar to that of conventional MOSFETs except that the metal gate electrode is removed in order to expose the underlying insulator to the electrolyte [3]. As a later development, the sensing film could also be integrated on top of a floating gate metal, giving rise to floating gate (FG) ion-sensitive devices [4]–[8].

In conventional ISFETs the transistor gate bias is applied through a reference electrode [3], [9]–[15]. However, inclusion of the bulky reference electrode poses challenges towards commercialization of ISFETs due to its dimension and CMOS incompatibility. Attempts to miniaturize the reference electrode were not successful due to the resulting drift and instability [16], [17].

In this paper, we present for the first time a highly sensitive and CMOS compatible solid state pH sensor integrated in the back-end-of-line (BEOL) of the standard 28 nm ultrathin body and buried oxide (UTBB) fully-depleted silicon-on-insulator (FDSOI) transistors with a front gate bias applied through a capacitive divider circuit. This provides (i) ultrahigh sensitivity arising from the fully depleted SOI feature,

2168-6734 © 2018 IEEE. Translations and content mining are permitted for academic research only.
Personal use is also permitted, but republication/redistribution requires IEEE permission.
See http://www.ieee.org/publications_standards/publications/rights/index.html for more information.

(ii) a capacitive divider circuit for front gate biasing through a control gate, (iii) CMOS compatibility by substituting the reference electrode with a control gate, (iv) tuning through back bias for operating-point optimization, and (v) better protection from the electrolyte.

The state-of-the-art CMOS downscaling and the ultralow power requirement need to address important issues such as electrostatic control, operating power consumption, and standby energy dissipation. The tuning (multi $V_{th}$) capability provided by the thin buried oxide (BOX) and highly doped ground plane [18]–[20] of UTBB architecture is accepted to solve these issues in the 28 nm and below FDSOI technology. The pH sensor reported in this paper is a first demonstration of an ISFET based on such UTBB industrial technology which is ideal for the IoT market and ultralow power systems.

Fabrication of the sensor in the BEOL is crucial for the state-of-the-art devices as direct exposure of the nearly 1.8 nm (EOT) gate oxide to the electrolyte would be detrimental to the device, and as stable operation of the sensor needs effective gate biasing (through a capacitive divider circuit).

This paper is organized in six sections where Section I is an introduction, and Section II describes the sensing mechanism. Section III discusses the UTBB FDSOI transistors' characterization and simulation of the pH sensor. In Section IV, fabrication and characterization of the extended gate pH sensor is presented. Section V describes fabrication and characterization of the sensor integrated in the BEOL. Finally, a concise conclusion is presented in Section VI.

## II. SENSING MECHANISM

It is generally considered that the surface charging mechanism for pH-sensing metal oxides is the preferential adsorption of protons or hydroxyl ions by surface hydroxyl groups to form positive or negative sites respectively [21]. Thus the resulting surface charge, which depends on an excess of one type of charged site over the other, is a function of the solution pH value. This phenomenon results in a surface potential which in turn causes a proton concentration gradient between the electrolyte bulk and surface (dielectric-electrolyte interface) that is mathematically described by Boltzmann equation as in (1) [22].

$$\left[H^{+}\right]_{S} = \left[H^{+}\right]_{B} \exp\left(\frac{-q\varphi}{k_{B}T}\right) \tag{1}$$

where $k_B$ is the Boltzmann constant, $q$ is the elementary charge, $T$ is temperature, $\varphi$ is surface potential, $[H^+]_B$ is the proton concentration in the bulk, and $[H^+]_S$ is the proton concentration at the surface.

Rearranging (1), the surface potential $\varphi$ is expressed as a function of the proton concentrations at the dielectric-electrolyte interface and in the bulk as given by (2) below, which is also referred to as the Nernst equation [12].

$$\varphi = \frac{k_{B}T}{q} \ln\left(\frac{\left[H^{+}\right]_{B}}{\left[H^{+}\right]_{S}}\right) \tag{2}$$

The pH sensitivity of the dielectric films is derived from (2) and is given mathematically as follows in (3).

$$\frac{d\varphi}{dpH} = -2.3\left(\frac{k_{B}T}{q}\right)\alpha \tag{3}$$

where $\alpha$ is the proton buffer capacity ($0 < \alpha < 1$).

## III. FDSOI ISFET CHARACTERISTICS

Developing the pH sensor based on UTBB FDSOI transistor, a sensitivity amplification is obtained arising from the strong electrostatic coupling between the two gates of the device [18]. The electrostatic coupling between the front gate and back gate is effective only in FDSOI transistors where the channel is ultrathin [23], [24]. In this case, a change of front gate voltage results in an amplified shift in threshold voltage at the back gate, because of the strong electrostatic coupling between the two gates [23]. The coupling factor ($\boldsymbol{\gamma}$) is given by (4) below for nMOS UTBB FDSOI devices.

$$\gamma = -\frac{\Delta V_{th}}{\Delta V_{g}} = \frac{C_{OX}}{C_{BOX}} \tag{4}$$

where $\Delta V_{th}$ is the shift in threshold voltage at the back gate, $\Delta V_g$ is a change in applied voltage at the front gate, $C_{OX}$ is the gate oxide capacitance, and $C_{BOX}$ is buried oxide capacitance.

Consequently, for FDSOI based ISFETs, the change in surface potential at the front gate is detected at the back gate amplified by the coupling factor ($\boldsymbol{\gamma}$), giving rise to an ultrahigh-sensitive solid state chemical sensor. Mathematically, it is shown in (5) below.

$$\Delta V_{th} = -\frac{C_{OX}}{C_{BOX}}\Delta\varphi \tag{5}$$

where $\Delta\varphi$ is the change in surface potential at the front gate.

The ISFET has been designed in which no reference electrode is needed due to the incorporation of a BEOL metal and a capacitively coupled control gate (CG). Hence, the front gate bias is applied through a control gate rather than a reference electrode. Therefore, this sensor is highly sensitive and CMOS compatible which is suited for low-power and low-cost ultrasensitive applications expected for the IoT market. The proposed approach has been validated by the consistent results obtained with simulation, proof-of-concept extended gate sensor, and BEOL integrated sensor fabrication and characterization.

The $I_D$-$V_{BG}$ characteristics of the UTBB FDSOI transistor at different gate voltages is shown on Fig. 1 below. The characteristics is in confirmation with the mathematical model presented in (4) and (5) that the shift in threshold voltage at the back gate is 13 times the change in front gate voltage which is equivalent to the ratio of gate oxide capacitance and BOX capacitance. Exploiting this special feature of the UTBB FDSOI, an amplified shift in voltage at the back gate corresponding to a small change in potential at the front gate is obtained. Moreover, the deep downscaled gate oxide (EOT = 1.8 nm) of the UTBB FDSOI makes this ISFET sensitive at single-charge resolution.

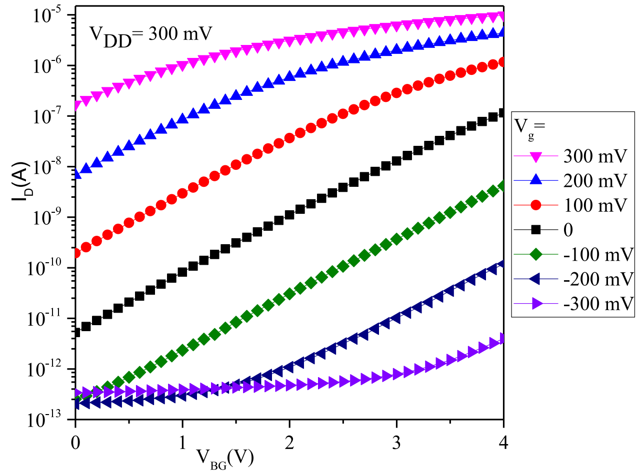


**FIGURE 1.** $I_D$-$V_{BG}$ **characteristics of the UTBB FDSOI transistor at different front gate voltages.**

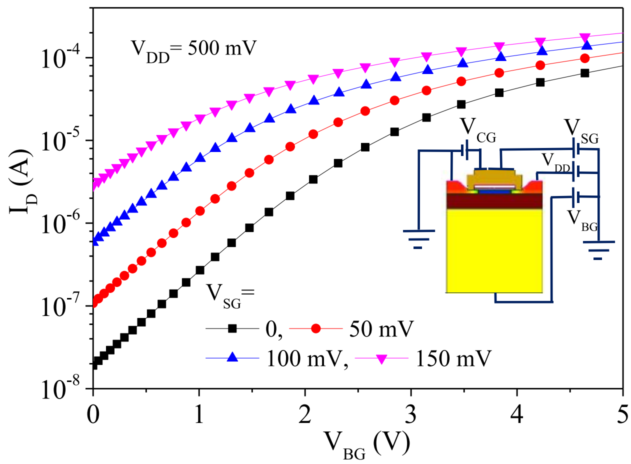


**FIGURE 2.** **Simulated** $I_D$-$V_{BG}$ **characteristics of the FDSOI ISFET at different surface potentials at the sensing gate (SG).**

Utilizing the S-Process simulation tool of TCAD Sentaurus, an n-type FDSOI transistor is designed having 25 nm BOX and 6 nm undoped silicon. The HKMG (high-$\kappa$ metal gate) structure of the device is defined by a 0.5 nm $SiO_2$ interlayer and a 3 nm thick $HfO_2$ on top of which a metal gate is deposited. Finally, the pH sensing film is deposited on top of the metal gate emulating the BEOL processing of the sensor.

For the electrical simulation, the source, drain, back gate, the floating gate, and the control gate were defined in S-Device tool. As there is no need of inserting trapped charges in the floating gate for sensing applications, zero net charges were set at the floating gate metal. A 500 mV biasing voltage was applied at the drain contact while the source and control gate were grounded. The result presented on Fig. 2 is obtained from the simulation.

From the simulation result of the pH sensor presented on Fig. 2, we can observe the theoretically expected shift in threshold voltage at the back gate which is amplified by 13 times for a corresponding change in voltage at the sensing gate (SG). This gives a maximum sensitivity of 775 mV/pH for a sensing film having a Nernstian pH response (59.6 mV/pH at room temperature).

## IV. THE EXTENDED GATE ISFET

As a proof of concept, we validated first the proposed approach as an extended gate pH sensor where the transistor and the pH sensing (transduction) component were connected through extended electrical connection. The schematic diagram of the extended gate sensor is shown on Fig. 3.

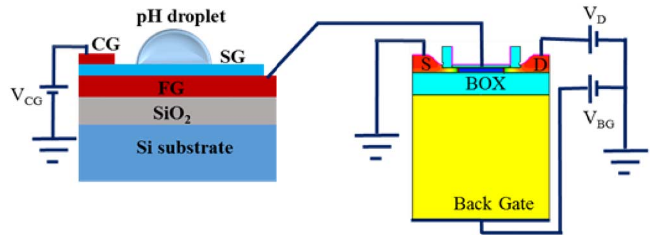


**FIGURE 3.** **Schematic diagram of the extended gate ISFET.**

The transduction component of the extended gate ISFET was processed isolated from the transistor. This fabrication process was therefore carried out on a 750 $\mu$m Si-substrate which had a thermally grown 500 nm $SiO_2$. A 10 nm/80 nm Ti/Pt metal layer was then deposited by E-beam evaporation on the substrate [22]. This metal layer serves as an extension of the FDSOI floating gate (FG) for extended gate operation of the ISFET. For the pH sensing, 50 nm aluminum oxide ($Al_2O_3$) was deposited by atomic layer deposition (ALD) on the Ti/Pt metal layer. Finally, 10 nm/80 nm Ti/Pt metal layer was deposited by E-beam evaporation for the control gate (CG).

This pH-sensor is based on the 28 nm UTBB FDSOI transistor manufactured by STMicroelectronics which has a channel of thickness, $t_{Si}$ = 6 nm, buried oxide (BOX) = 25 nm, and equivalent gate oxide thickness = 1.8 nm. The device has a gate width and gate length of 80 nm and 1 $\mu$m respectively. External electrical connections were made between the floating gate (FG) of transduction component and front gate of the transistor for pH-sensitivity characterizations.

The sensitivity characterization of the extended gate ISFETs were carried out at 3- different pH values: at pH 6, pH 7.3, and pH 8. This characterization pH range is sufficient for biomedical applications such as acidity monitoring of blood, and pH measurement of saliva [25]. However, the sensor can be operated in wider pH range as both the sensing film and the transistor have wide linear operating ranges [10], [18].

The protocol used to characterize the sensor's sensitivity is briefly described here. Exactly the same protocol (with different pH solutions) has been exploited for the BEOL ISFETs described in Section V. Before starting the pH-sensing characterization, the samples were cleaned with

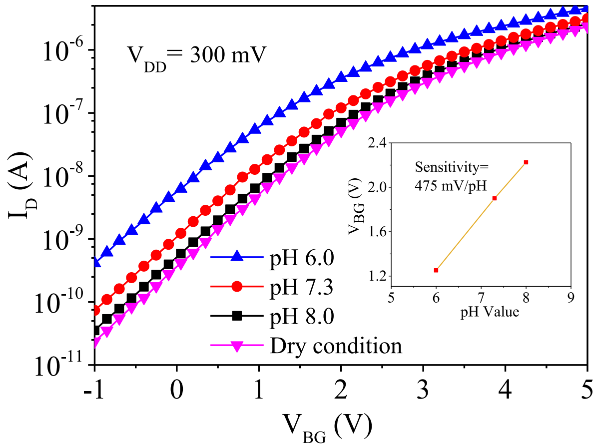


**FIGURE 4.** pH sensitivity of the extended gate ISFET.

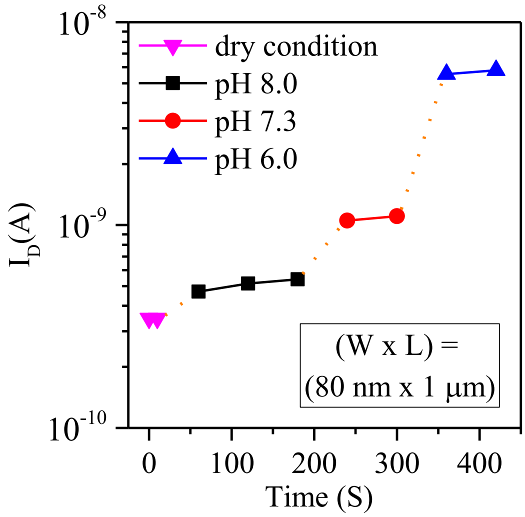


**FIGURE 5.** Chronogram of the extended gate pH sensor.

acetone-isopropanol-deionized water and dried with nitrogen. The pH solutions were then dispensed on the sensing area, and $I_D$-$V_{BG}$ sweeps were taken in 1, 2, and 3 minutes. The tests were started at the highest pH (pH 8.0 in this case), continued with pH 7.3, and finally to pH 6.0. After finishing electrical measurements with each pH solution, the droplet is removed from the sensor using a micropipette. The volume of solution dispensed on sensor was 30 μl.

In the extended gate pH sensor, a pH-sensitivity of 475 mV/pH is obtained which is superior performance with respect to the state-of-the-art ISFETs. This experimental sensitivity is less than the simulation result (ideally maximum sensitivity) which can be justified by the sub-Nernstian response of the sensing film and the signal loss on the external electrical connections between the transistor and the transduction component.

In addition to the high sensitivity, the design of biasing through a capacitive divider circuit, makes the sensor CMOS compatible by getting rid of the bulky reference electrode. The very high $I_{ON}/I_{OFF}$ ratio of the UTBB FDSOI industrial transistor provides with a wide linear operating range and high signal to noise ratio (SNR).

At the different pH values, measurements were repeated to assess repeatability and stability. From such measurements, very good repeatability and stability were observed during the first 3-minutes which is a remarkable performance compared to the work on literature [26] where initial drift was observed for 1 hour. The chronogram of the extended gate pH sensor is presented on Fig. 5 that shows a stable and fast pH-response.

## V. ISFET INTEGRATED IN THE FDSOI BEOL

After the proof-of-concept validation with the extended gate pH sensor, prototypes of the proposed pH sensor with the sensing gate and control gate in the BEOL of industrial UTBB FDSOI transistors have been fabricated. The BEOL integrated ISFETs were fabricated based on the FDSOI transistor having the same specification as in the extended gate ISFET. The schematic diagram of the ISFET integrated in BEOL is shown below on Fig. 6.

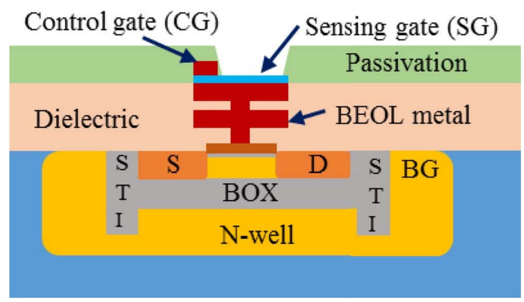


**FIGURE 6.** Schematic diagram of the BEOL integrated ISFET.

The following process flow is followed for the fabrication of the pH sensor in BEOL. 50 nm of $Al_2O_3$ deposited by ALD is used as pH-sensing film.

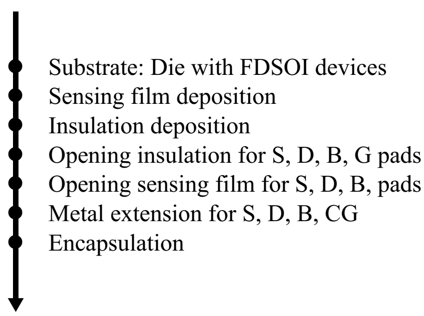


The sensing area (sensing gate) of the BEOL integrated ISFET has an area of 29 μm × 70 μm. The electrical connection schematics of the sensors (9 sensors per die), and the optical image of the fabricated sensor are shown below on Fig. 7.

The scanning electron microscope (SEM) image of the sensor's cross section across the sensing gate and the control gate is also presented below on Fig. 8.

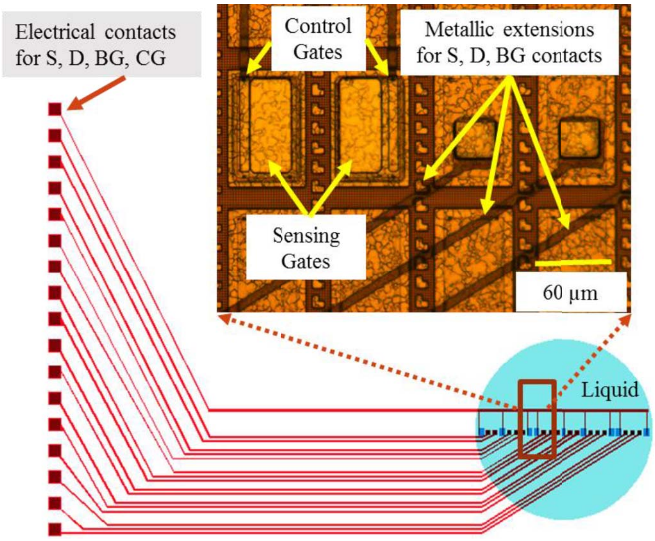


FIGURE 7. Layout of the sensors on the die and optical image of the BEOL integrated ISFETs.

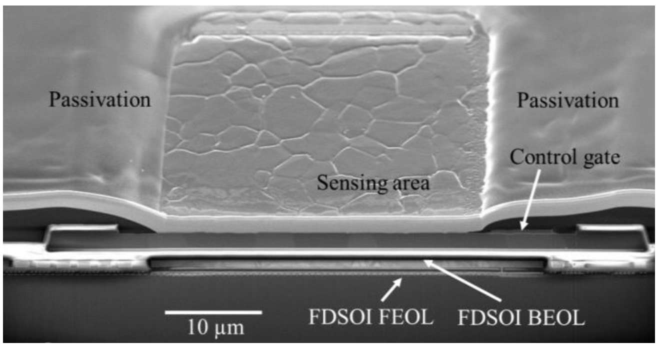


FIGURE 8. SEM image of the sensor's cross section.

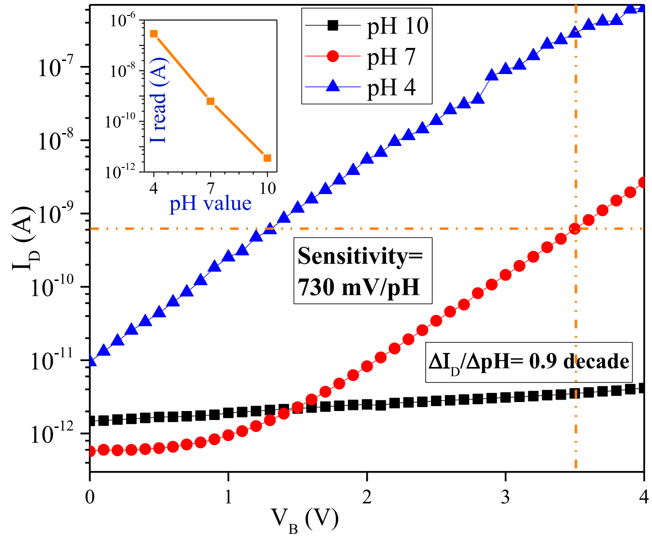


FIGURE 9. pH sensitivity of the BEOL integrated ISFET [28].

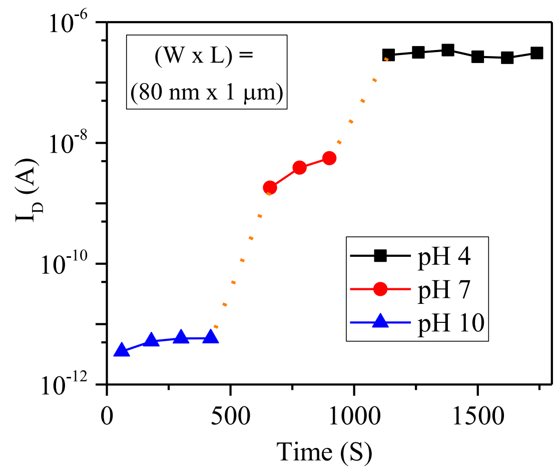


FIGURE 10. Chronogram of the BEOL integrated pH sensor.

Characterizing the pH sensor which is integrated in BEOL of the 28 nm UTBB FDSOI, at wider pH range (pH 4 to pH 10) than the range utilized for the proof of concept extended gate sensor, a sensitivity of 730 mV/pH is obtained. This sensitivity is in confirmation with both the theoretically expected value and the simulation result.

The highly enhanced sensitivity and the steep subthreshold slope make the performance of this sensor suited for both fixed voltage and fixed current readout circuits. The experimental sensitivity which is 12-times higher than the Nernst limit is presented on Fig. 9. The pH-10 curve, which has very close similarity with the curve on Fig. 1 at $V_g = -300$ mV, can be explained by the relatively stronger accumulation regime due to the higher negative potential at the sensing gate resulting from the higher pH value. Such operating regimes can however be compensated by a proper back gate biasing as can be observed on Fig. 1.

On Fig. 10 we present the chronogram of the sensor which we integrated in the BEOL. From this figure, we can observe the demonstrated fast response time and very good stability. Stable pH sensing results were obtained in less than 1-minute and without conditioning the sensing film which is a significant performance improvement compared to literature reports [3], [27].

Benchmarked with state-of-the-art, the developed pH sensor demonstrates superior sensitivity. Not only in terms of sensitivity, this sensor has also remarkably better performances in terms of CMOS compatibility and scaling as

TABLE 1. Benchmark with state-of-the-art ISFETs [8], [14], [29], [30] ( *REF: reference electrode, CG: control gate)*.

| Parameter | [8] | [14] | [29] | [30] | This work | |
|---|---|---|---|---|---|---|
| | | | | | Simulation | pH Sensor in BEOL |
| Sensitivity (mV/pH) | 58 | 453 | 103.8 | 123.8 | 775 | 730 |
| Gate bias | N/A | REF | REF | REF | CG | CG |
| Substrate | Bulk | SOI | Bulk | Bulk | FDSOI | FDSOI |
| Devices per sensor | 2 | 1 | 8 | 8 | 1 | 1 |
| Technology node | 0.35 μm | 0.18 μm | 0.18 μm | 65 nm | 28 nm | 28 nm |

it avoids the bulky reference electrode and because it is developed based on a deeply downscaled technology node.

## VI. CONCLUSION

Integrating aluminum oxide ($Al_2O_3$) sensing gate on the gate metal of industrial UTBB FDSOI transistors in BEOL, ultrahigh-sensitive and CMOS compatible ISFETs are fabricated. We demonstrated an experimental sensitivity of 730 mV/pH which is 12 times higher than the Nernst limit. The front gate bias through a capacitively coupled control gate of the capacitive divider circuit enables highly stable ISFET performance and CMOS compatibility. The steep subthreshold slope of the sensor makes it suited for both fixed bias and fixed current readout circuits. The ISFET can also operate at a supply voltage down to 100 mV for the transducer, on sensing area as small as 29 $\mu$m $\times$ 70 $\mu$m providing a huge advantage for small-size, low-power, and low-cost requirements of the rapidly growing IoT market.

## ACKNOWLEDGMENT

Région Auvergne Rhône-Alpes is acknowledged for a Coopera project funding.

## REFERENCES

[1] P. Bergveld, "Development of an ion-sensitive solid-state device for neurophysiological measurements," *IEEE Trans. Biomed. Eng.*, vol. BME-17, no. 1, pp. 70–71, Jan. 1970.

[2] R. G. Kelly, "Microelectronic approaches to solid state ion selective electrodes," *Electrochimica Acta*, vol. 22, no. 1, pp. 1–8, 1977.

[3] H. Abe, M. Esashi, and T. Matsuo, "ISFET's using inorganic gate thin films," *IEEE Trans. Electron Devices*, vol. ED-26, no. 12, pp. 1939–1944, Dec. 1979.

[4] N. Y. Shen, Z. Liu, B. A. Minch, and E. C. Ken, "The chemoreceptive neuron MOS transistors (C/spl nu/MOS): A novel floating-gate device for molecular and chemical sensing," in *Proc. 12th Int. Conf. TRANSDUCERS Solid-State Sens. Actuators Microsyst.*, vol. 1, 2003, pp. 69–72.

[5] J. van der Spiegel, I. Lauks, P. Chan, and D. Babic, "The extended gate chemically sensitive field effect transistor as multi-species microprobe," *Sensors Actuators*, vol. 4, pp. 291–298, Jan. 1983.

[6] J. Bausells, J. Carrabina, A. Errachid, and A. Merlos, "Ion-sensitive field-effect transistors fabricated in a commercial CMOS technology," *Sensors Actuators B Chem.*, vol. 57, nos. 1–3, pp. 56–62, 1999.

[7] L. Rahhal *et al.*, "High sensitivity pH sensing on the BEOL of industrial FDSOI transistors," *Solid-State Electron.*, vol. 134, pp. 22–29, Aug. 2017.

[8] J. M. Rothberg *et al.*, "An integrated semiconductor device enabling non-optical genome sequencing," *Nature*, vol. 475, no. 7356, pp. 348–352, 2011.

[9] T. Matsuo and K. D. Wise, "An integrated field-effect electrode for biopotential recording," *IEEE Trans. Biomed. Eng.*, vol. BME-21, no. 6, pp. 485–487, Nov. 1974.

[10] T. Matsuo and M. Esashi, "Methods of ISFET fabrication," *Sensors Actuators*, vol. 1, pp. 77–96, Jan. 1981.

[11] R. P. Buck, D. E. Hackleman, and W. R. Kenan, "Field effect potentiometric sensors," *Anal. Chem.*, vol. 49, no. 14, pp. 2315–2321, 1977.

[12] M. Spijkman *et al.*, "Beyond the Nernst-limit with dual-gate ZnO ion-sensitive field-effect transistors," *Appl. Phys. Lett.*, vol. 98, no. 4, 2011, Art. no. 043502.

[13] H.-J. Jang and W.-J. Cho, "Performance enhancement of capacitive-coupling dual-gate ion-sensitive field-effect transistor in ultra-thin-body," *Sci. Rep.*, vol. 4, Jun. 2014, Art. no. 5284.

[14] Y.-J. Huang *et al.*, "High performance dual-gate ISFET with non-ideal effect reduction schemes in a SOI-CMOS bioelectrical SoC," in *Proc. IEEE Int. Electron Devices Meeting (IEDM)*, Washington, DC, USA, 2015, pp. 29.2.1–29.2.4.

[15] K. B. Parizi, A. J. Yeh, A. S. Y. Poon, and H. S. P. Wong, "Exceeding nernst limit (59mV/pH): CMOS-based pH sensor for autonomous applications," in *Proc. Int. Electron Devices Meeting*, San Francisco, CA, USA, 2012, pp. 24.7.1–24.7.4.

[16] J. Janata, "Historical review. Twenty years of ion-selective field-effect transistors," *Analyst*, vol. 119, no. 11, pp. 2275–2278, 1994.

[17] C. Toumazou and P. Georgiou, "Piet Bergveld—40 years of ISFET technology: From neuronal sensing to DNA sequencing," *Electron. Lett.*, vol. 47, no. 26, pp. S7–S12, Dec. 2011.

[18] T. Skotnicki and S. Monfray, "UTBB FDSOI: Evolution and opportunities," in *Proc. 45th Eur. Solid-State Device Research Conf. (ESSDERC)*, 2015, pp. 76–79.

[19] L. Grenouillet *et al.*, "UTBB FDSOI transistors with dual STI for a multi-Vtstrategy at 20nm node and below," in *Proc. IEEE Int. Electron Devices Meeting (IEDM)*, San Francisco, CA, USA, 2012, pp. 3.6.1–3.6.4.

[20] J.-P. Noel *et al.*, "Multi-$V_T$ UTBB FDSOI device architectures for low-power CMOS circuit," *IEEE Trans. Electron Devices*, vol. 58, no. 8, pp. 2473–2482, Aug. 2011.

[21] D. E. Yates, S. Levine, and T. W. Healy, "Site-binding model of the electrical double layer at the oxide/water interface," *J. Chem. Soc. Faraday Trans. 1 Phys. Chem. Condens. Phases*, vol. 70, pp. 1807–1818, 1974.

[22] G. T. Ayele *et al.*, "Development of ultrasensitive extended-gate Ion-sensitive-field-effect-transistor based on industrial UTBB FDSOI transistor," in *Proc. 47th Eur. Solid-State Device Res. Conf. (ESSDERC)*, 2017, pp. 264–267.

[23] H.-K. Lim and J. G. Fossum, "Threshold voltage of thin-film silicon-on-insulator (SOI) MOSFET's," *IEEE Trans. Electron Devices*, vol. ED-30, no. 10, pp. 1244–1251, Oct. 1983.

[24] D.-I. Moon, J.-W. Han, and M. Meyyappan, "Comparative study of field effect transistor based biosensors," *IEEE Trans. Nanotechnol.*, vol. 15, no. 6, pp. 956–961, Nov. 2016.

[25] S. Baliga, S. Muglikar, and R. Kale, "Salivary pH: A diagnostic biomarker," *J. Indian Soc. Periodontol.*, vol. 17, no. 4, pp. 461–465, 2013.

[26] P. Bergveld, "Development, operation, and application of the ion-sensitive field-effect transistor as a tool for electrophysiology," *IEEE Trans. Biomed. Eng.*, vol. BME-19, no. 5, pp. 342–351, Sep. 1972.

[27] L.-C. Yen, M.-T. Tang, C.-Y. Tan, T.-M. Pan, and T.-S. Chao, "Effect of sensing film thickness on sensing characteristics of dual-gate poly-Si ion-sensitive field-effect-transistors," *IEEE Electron Device Lett.*, vol. 35, no. 12, pp. 1302–1304, Dec. 2014.

[28] G. T. Ayele *et al.*, "Ultrahigh-sensitive and CMOS compatible ISFET developed in BEOL of industrial UTBB FDSOI," in *Proc. IEEE Symp. VLSI Technol.* 2018, pp. 97–98.

[29] X. Huang *et al.*, "A 64×64 1200fps CMOS ion-image sensor with suppressed fixed-pattern-noise for accurate high-throughput DNA sequencing," in *VLSI Circuits Dig. Tech. Papers Symp.*, 2014, pp. 1–2.

[30] Y. Jiang *et al.*, "A 512×576 65-nm CMOS ISFET sensor for food safety screening with 123.8 mV/pH sensitivity and 0.01 pH resolution," in *Proc. IEEE Symp. VLSI Technol.*, Honolulu, HI, USA, 2016, pp. 1–2.

**GETENET TESEGA AYELE** received the B.Sc. degree in electrical engineering from Hawassa University, Ethiopia, in 2009, the M.Sc. degree in electrical power engineering from Addis Ababa University, Ethiopia, in 2011, and the M.Sc. degree in nano and bio-photonics from ENS Cachan, France, and the Wroclaw University of Technology, Poland (Erasmus program), in 2015. He is currently pursuing the Ph.D. degree on development of CMOS chemical sensors with STMicroelectronics, France, INSA Lyon, France, and Université de Sherbrooke, Canada, in co-supervision.

**STEPHANE MONFRAY** is the Principal Scientist with the Silicon Technologies Development-Silicon Photonics Group, STMicroelectronics, Crolles. Since 2008, he has been a member of the STMicroelectronics expert's staff. He was involved in FP6 and FP7 projects (Nanocmos, Pullnano, Duallogic, and COMPOSE3) and leads since 2012 a national project (FUI) on energy harvesting. He has authored and co-authored over 70 publications in major conferences and journals, of over 30 patents, of a book chapter. He was an instructor at the SOI conference short course in 2010, and at MIGAS in 2011, and he had multiple participations and paper presentations at the IEDM in 2001, 2002, 2004, 2007, and 2010. He was a co-recipient of the Paul Rappaport Award in 2000 and the 2012 French Electronic Grand Prize "General Ferrié" for his work on thin film devices.

**SERGE ECOFFEY** received the master's degree in material science and the Ph.D. degree in electrical engineering from the Swiss Federal Institute of Technology Lausanne in 2001 and 2007, respectively. Since 2009, he has been with the Université de Sherbrooke, Sherbrooke, QC, Canada, where he became an Adjunct Professor in 2012. His research focuses on microfabrication, nanoelectronic devices, MEMS, and the development of chemical planarization processes.

**FRÉDÉRIC BOEUF** was born in 1972. He received the M.Eng. and M.Sc. degrees from the Institut National Polytechnique de Grenoble in 1996 and the Ph.D. degree from the University Joseph Fourier, Grenoble, France, in 2000. Then he joined STMicroelectronics working on Advanced Devices Physics and Integration. He has authored and co-authored over 150 technical papers. He is currently managing the Silicon Photonics, BiCMOS, and Advanced Devices Technology group inside STMicroelectonics Silicon Development Group.

**JEAN-PIERRE CLOAREC** received the Ph.D. degree in material engineering from the Ecole Centrale de Lyon in 1997, where he is a Professor. He is a member of the Lyon Institute of Nanotechnology. His research interests focus on surface functionalization and molecular interactions at solid/liquid interface.

**DOMINIQUE DROUIN** (M'10) received the bachelor's degree in electrical engineering and the Ph.D. degree in mechanical engineering from the Université de Sherbrooke, Sherbrooke, QC, Canada, in 1994 and 1998, respectively, where he has been a Professor with the Electrical and Computer Engineering Department since 1999. He is a holder of NSERC/IBM Industrial Research Chair on Smarter Microelectronics Packaging for Performance Scaling. He has expertise in the fields of nanoelectronics (RRAM, TFT, MM, and sensors) and materials characterization (SEM, CL, EDX, and XPS).

**ABDELKADER SOUIFI** received the Ph.D. degree in microelectronics from the National Institute of Applied Sciences (INSA Lyon) in 1993. From 1994 to 1995, he was with the Institute of Thin Films, Julich Research Center, Germany, where he was involved in the studies of nanostructures for silicon-based nanodevices. In 1995, he joined INSA Lyon as an Assistant Professor in the field of heterojunction-based devices. Since 1998, the research activities on silicon-based nanoelectronics have been developed. He got a Full Professor position in 2002 and led the Silicon Electron Device Group with the Lyon Institute of Nanotechnology from 2002 to 2007. Since 2008, he has been engaged in the international CNRS Lab, University de Sherbrooke, Sherbrooke, QC, Canada (UMI-LN2). His current research interests include the nanofabrication and characterizations of ultralow power electron devices and sensors.